15th Triennial World Congress, Barcelona, Spain

INDUSTRIAL APPLICATIONS OF PREDICTIVE ADAPTIVE CONTROL BASED ON MULTIPLE IDENTIFIERS

J. M. Lemos * **E. Mosca** ** **R. N. Silva** *** **P. O. Shirley** ****

* *INESC-ID, R. Alves Redol, 9, Lisboa, Portugal*
** *Dip. Sistemi e Informativa, Via S. Marta, 3, Firenze, Italia*
*** *Fac. Ciências e Tecnologia, UNL, MOnte da Caparica, Portugal*
**** *U. Aberta de Lisboa and INESC-ID, Lisboa, Portugal*

Abstract: Experimental results on industrial applications of the MUSMAR adaptive Predictive Controller are reported in this paper. They concern superheated steam temperature control in a thermoelectric power unit, oil temperature control in a distributed collector solar field, and trailing center line rate of cooling in a arc welding process. The processes considered are described, with an emphasis on the explanation of the difficulties met in the control problems associated to them. It is stressed that the examples presented in the paper are all based on experiments performed on actual full scale plants. *Copyright ©2002 IFAC.*

Keywords: Adaptive Control, Process Control, Predictive Control, Energy, Electric Power Systems, Solar Energy, Welding.

1. INTRODUCTION.

The MUSMAR algorithm embodies an adaptive predictive controller developed in tight connection with LQ stochastic control. Although only a local convergence theory is available, a number of properties have shown to hold under typical operating conditions of process control applications. While some properties are common to other adaptive predictive controllers, others are peculiar to MUSMAR, making it a powerful tool for process control. In particular, the use of multiple identifiers, embodied in MUSMAR, proves to be a key feature in this respect. By multiple identifiers it is understood that the control synthesis and adaptation mechanism does not rely on a single model. Instead, a set of models separately estimated from plant data and suitably combined are used for control synthesis. The redundancy thereby introduced is a keystone for MUSMAR properties.

This paper presents and discusses experimental case studies performed with MUSMAR in three different industrial plants. They concern superheated steam temperature control in a thermoelectric power unit, oil temperature control in a distributed collector solar field, and trailing center line rate of cooling in a arc welding process.

The processes considered are described, with an emphasis on the explanation of the difficulties met in the control problems associated to them. These include unmodelled dynamics, uncertain and varying long input/output transport delay, colored noise, nonlinear effects, unpredictable changes in dynamics and fast acting strong disturbances due to stochastic loads. By means of experimental results it is shown how MUSMAR is able of tackling these difficulties leading to an increased performance when compared to other control techniques. In what concerns the superheated steam temperature process, it is shown that, with respect to an optimized standard controller, MUSMAR yields a reduction by a factor of 3 of the fluctuations around the set-point. Furthermore, MUSMAR equipped with feed-forward from accessible disturbances is capable to tackle efficiently fast load changes. In what concerns the distributed collector solar field, it is shown how a cascade of MUSMAR

[1] Part of this work has been done under POSI/SRI/36328 and under POSI, IIIrd EC Framework Program.

controllers operating at different sampling rates is capable to tackle a very long and time varying plant transport delay. Finally, for the welding process, it is shown that it is not possible to find a unique linear controller which is able to stabilize the whole class of possible plant outcomes. This is made by applying a simple robust stability result to experimental estimates of plant uncertainty and motivates the use of adaptive control. Opposite to what happens when PID or pole placement controllers are used, MUSMAR yields a satisfactory performance. It is stressed that the examples presented in the paper are all based on experiments performed on actual full scale plants.

2. THE MUSMAR ADAPTIVE PREDICTIVE CONTROLLER.

The MUSMAR controller (Greco *et al.*, 1984; Mosca, 1995) is based on a number of separately estimated predictive models. In the presence of plant/model mismatches, such as the situations found here, the redundancy thereby introduced proves important for achieving a correct control action (Mosca *et al.*, 1989). This multiple model approach is a distinctive feature with respect to other approaches to predictive adaptive control, relying on the adaptation of a single model from which others are then obtained.

In (Greco *et al.*, 84, 1984) it is shown that MUSMAR is equivalent to a bank of parallel self-tuners, each one tuned to a different value of plant delay and with different weights. If the actual plant delay is bigger than the delay assumed for a given self-tuning channel the corresponding weight will be zero. Insensitivity to uncertainty in plant delay is thus achieved up to some degree.

2.1 *MUSMAR algorithm*

The MUSMAR algorithm (Greco *et al.*, 84, 1984) reads as follows:

At the beginning of each sampling interval t (discrete time), recursively perform the following steps:

1.Sample plant output, $y(t)$ and compute the tracking error $\tilde{y}$, with respect to the desired set-point $y^*(t)$, by:

$$\tilde{y}(t) = y^*(t) - y(t) \tag{1}$$

2.Using Recursive Least Squares (RLS), update the estimates of the parameters θ_j, ψ_j, μ_{j-1} and ϕ_{j-1} in the following set of predictive models:

$$\tilde{y}(t+j) \approx \theta_j u(t) + \psi_j' s(t) \tag{2}$$

$$u(t+j-1) \approx \mu_{j-1} u(t) + \phi_{j-1}' s(t) \tag{3}$$

$$j = 1, \ldots, T$$

where $\approx$ denotes equality in least squares sense and $s(t)$ is a sufficient statistic for computing the control, hereafter referred as the pseudo-state, given by

$$s(t) = [\tilde{y}(t) \, \ldots \, \tilde{y}(t-n+1) \; u(t-1) \, \ldots \, u(t-m) \; w_1(t) \ldots w_1(t-n_{w1}) \ldots w_N(t) \ldots w_N(t-n_{wN}) \; 1]' \tag{4}$$

where the w_i are samples of auxiliary variables such as intermediate process variables or accessible disturbances. Since, at time t, $\tilde{y}(t+j)$ and $u(t+j)$ are not available for $j \geq 1$, for the purpose of estimating the parameters, the variables in (2,3) are delayed in block of T samples. The estimation equations are thus,

$$K(t) = \frac{P(t-1)\varphi(t-T)}{1 + \varphi'(t-T)P(t-1)\varphi(t-T)[1-\beta(t)]} \tag{5}$$

$$P(t) = [I - K(t)\varphi'(t-T)(1-\beta(t))]P(t-1) \tag{6}$$

and, for $j = 1, \ldots, T$:

$$\hat{\Theta}_j(t) = \hat{\Theta}_j(t-1) + K(t)[y(t-T+j) - \hat{\Theta}_j(t-T)'\varphi(t-T)] \tag{7}$$

for $j = 1, \ldots, T-1$:

$$\hat{\Omega}_j(t) = \hat{\Omega}_j(t-1) + K(t)[u(t-T+j) - \hat{\Omega}_j(t-T)'\varphi(t-T)] \tag{8}$$

In these equations, $\hat{\Theta}_j$ represents the estimate of the parameter vector of the output predictors, given at each discrete time and for each predictor j by

$$\hat{\Theta}_j = [\theta_j \;\; \psi_j']'$$

and $\varphi(t-T)$ represents the regressor, common to all predictors, given by

$$\varphi(t-T) = [u(t-T) \; s'(t-T)]'$$

Similarly, $\hat{\Omega}_j$ represents the estimate of the parameter vector of the input predictors, given at each discrete time and for each predictor j by

$$\hat{\Omega}_j = [\mu_j \;\; \phi_j']'$$

Note that, since the regressor $\varphi(t-T)$ is common to all the predictive models, the Kalman gain update (5) and the covariance matrix update (6) are also common to all the predictors and need to be performed only once per time iteration. This greatly reduces the computational load.

The variable $\beta(t)$ denotes the quantity of information discarded in each iteration, being given according to a directional forgetting (Kulhavý, 1987) scheme by

$$\beta(t) = 1 - \lambda + \frac{1-\lambda}{\varphi'(t-T)P(t-1)\varphi(t-T)}$$

where λ is a constant to be chosen between 0 (complete forgetting) and 1 (no forgetting) which determines the rate of forgetting in the direction of incoming information. In practice, a factorized version is used to implement eq. (5).

3.Apply to the plant the control given by

$$u(t) = f's(t) + \eta(t) \tag{9}$$

where η is a white dither noise of small amplitude and f is the vector of controller gains, computed from the estimates of the predictive models by

$$f = -\frac{1}{\alpha}\left(\sum_{j=1}^{T} \theta_j \psi_j + \rho \sum_{j=1}^{T-1} \mu_j \phi_j\right) \tag{10}$$

with the normalization factor α given by

$$\alpha = \sum_{j=1}^{T} \theta_j^2 + \rho(1 + \sum_{j=1}^{T-1} \mu_j^2) \qquad (11)$$

2.2 *Guidelines for MUSMAR configuration.*

The choice of the variables and the number of their past samples entering $s(t)$ defines the structure of the controller. The choice of n and m should be such that it allows to capture the dominant dynamics of the system. Too big values of n and m imply more parameters to estimate and this may lead to identifiability problems, in turn causing loss of control performance. Due to the separate estimation of the predictive models, MUSMAR is able to tackle the situation in which the controller gains are to be tuned in the (local) minimum of a steady state quadratic cost, constrained to the *a priori* chosen controller structure (Mosca *et al.*, 89, 1989). The pseudo-state $s(t)$ also includes samples of auxiliary variables. The best choice for the number of samples in each of these samples is found in each case by trial and error, first in simulation and then adjusted according to plant experiments. The value of the prediction horizon T should be large enough so that the gains are close approximations to steady-state (infinite horizon) LQ optimal gains. However, if T is too large, predictive model parameter estimates loose accuracy and this results in gain de-tuning and consequent loss of performance. A trade-off has thus to be made for choosing T.

3. SUPERHEATED STEAM TEMPERATURE CONTROL.

Tests on superheated steam temperature control have been conducted at the Barreiro thermoelectric power plant of CPPE (Companhia Portuguesa de Produção de Electricidade/EDP Group). The steam coming from the boiler drum passes through the low temperature superheater (LTSH) and receives a spray water injection before passing through the high temperature superheater (HTSH) to the steam collector. From the collector, the steam is extracted for use, either by the turbine or by industrial users. These induce frequent and unexpected load changes in their normal mode of operation. The process variable to be controlled is $y = T_{vsato}$, the steam temperature at the output of HTSH. The manipulated variable is $u = C_{vgij}$, the command of the spray water valve, which influences the spray water flow, C_{gij}. When the spray water valve opens, the flow C_{gij} increases and the steam temperature decreases. The measure T_{vsati} of steam temperature after spray water injection and before the HTSH is available and is used for feedback. The action of the manipulated variable on T_{vsati} is fast. The influence of a change of T_{vsati} on T_{vsato} is much slower. This dynamics is influenced by the load imposed on the system, the super heated steam flow, C_{vsato}. Both C_{vsato} and the inflow of air to the furnace, C_{afrn}, disturb the system.

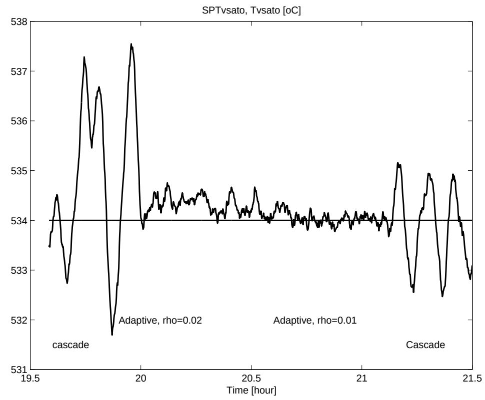

Fig. 1. Superheated steam: Steam temperature.

The standard control structure consists of a PI/PID cascade controller with feed-forward. The inner loop (with faster dynamics) controls T_{vsati} by manipulating the valve command, C_{vgij}. The outer loop (slower) controls T_{vsato} by manipulating the set-point of the inner loop. This set point is also affected by the accessible disturbance measurements of steam flow, C_{vsato}, and fuel flow, C_{cfrni}.

3.1 *Superheated steam: Experimental results.*

Figs. 1 up to 3 document an experiment performed with MUSMAR on the superheated steam plant. Fig. 1 shows (above) the superheated steam temperature superimposed on the set-point of 534^oC and (below) the command signal of the spray water signal (manipulated variable, expressed in percentage of opening with 0% corresponding to valve closed and 100% to valve fully open). Time is in $[hour]$. MUSMAR parameters were selected according to: $T = 15$, $n = 3$, $m = 2$, and $\lambda = 0.998$. The sampling period was selected at $5\,s$. The standard deviation of the dither noise η is 1% of the maximum opening of the valve. Initially, $\rho = 0.02$. Besides the samples of the plant output and manipulated variable, the pseudo-state also includes as auxiliary variables one sample of T_{vsati} (steam temperature after the spray water injection and before the superheater), and the last two measured samples of C_{vsato} (flow of steam) and C_{afrni} (flow of air at the input of the furnace). Experiments revealed that the inclusion of these auxiliary variables, which actually provide an adaptive feed-forward effect, is of paramount importance for obtaining a good performance. In this respect, it should be kept in mind that steam flow is usually continuously varied by industrial users.

The experiment starts with the standard cascade controller connected. At 19.85 h the adaptive controller is turned on. After a startup transient due to adaptation, the gains are adjusted so that a noticeable reduction

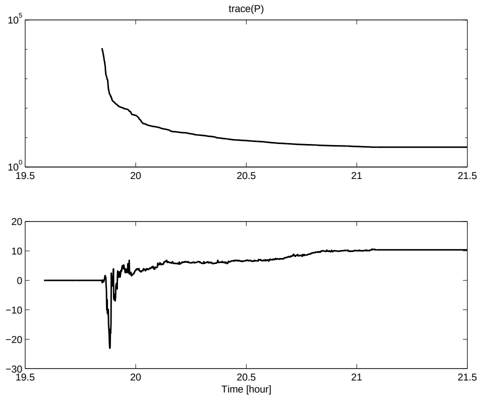

Fig. 2. Superheated steam: Trace of the covariance matrix and one controller gain.

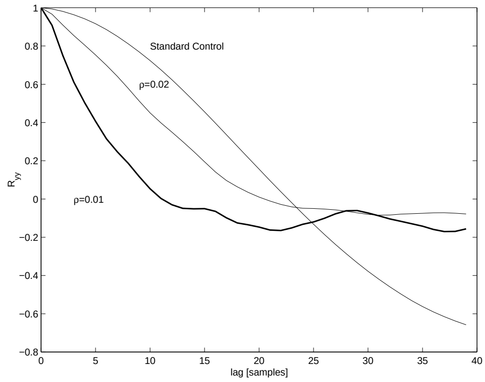

Fig. 3. Superheated steam: Output temperature autocorrelation.

in temperature fluctuations is observed. This happens despite persistent and strong disturbances due to the steam flow variations.

The startup transient is readily seen in fig. 2. This figure shows the trace of the covariance matrix of the RLS identifiers (above, in logarithmic units) and one of the controller gains (below). At 20.7 h ρ was reduced to 0.01 and the controller gains were adjusted, as seen in fig. 2. This resulted in a closer set-point tracking but with increased variation of the manipulated variable, which passed from $E[u^2] = 4.4$ with $\rho = 0.02$ to $E[u^2] = 6.1$ with $\rho = 0.01$. At 21.1 h adaptive control was disconnected, standard control was applied again and temperature fluctuations greatly increased. It is interesting to look at the autocorrelation function of the output temperature signal in the three segments when $\rho = 0.02$, when $\rho = 0.01$ and the last segment in which standard control is applied. These are seen in fig. 3. The autocorrelation when standard control is used clearly indicates an oscillatory behavior. Temperature samples well separated in time have a strong correlation and this indicates that control can be improved by taking advantage of this fact. When MUSMAR with $\rho = 0.02$ is applied, the autocorrelation decays monotonically, faster then in the previous case, and then stays close to zero. The same happens when $\rho = 0.01$, but the decay is now even faster. In the ideal case where the steam temperature is an uncorrelated signal (added to a constant) no further improvements in tracking the set-point would be possible. This situation would correspond to $\rho = 0$ and a convenient choice of the pseudo-state orders. By using the method described in (Harris, 1989) it is possible to estimate how far the various situations are from ideal minimum variance. Applying this procedure it is found that the ratio of temperature measured variance to ideal minimum variance is: 417 with standard control, 22 with MUSMAR, $\rho = 0.02$ and 7 with MUSMAR, $\rho = 0.01$. It should be stated that ideal minimum variance is not acceptable because it would lead to an excessive control action, resulting in valve wearing. Instead MUSMAR $\rho = 0.01$ leads to a control action which is considered completely acceptable by plant operating staff.

4. CASCADE CONTROL IN A SOLAR FIELD.

Cascade control is a classical structure in process control. It explores the situation in which the system to be controlled can be split in two series subsystems P_1 and P_2 with the dominant time constant of P_1 being much faster than the dominant time constant of P_2. Two controllers C_1 and C_2 are connected such that the manipulated variable of C_2, u_2, is the set-point of C_1, thus forming two nested loops. Furthermore, in a computer control framework, again exploring the difference between the dominant time constants of P_1 and P_2, these subsystems are sampled at different rates h_1 and h_2, with $h_2 > h_1$. In this example, experimental results are presented on the application of a cascade control structure to the oil outlet temperature in a distributed collector solar field. Both loops of the cascade employ MUSMAR. The use of MUSMAR together with the above mentioned multi-rate sampling scheme provides an alternative way of controlling this plant which is particularly effective in the outer loop where a long, time varying, pure delay is present. The plant to be controlled consists of a distributed solar collector field (manufactured from ACUREX) which is part of Plataforma Solar de Almeria, located in the south of Spain. The field is made of 480 cylindric collectors of parabolic type, which concentrate the solar radiation in a metallic pipe located along their focus. The metallic pipe contains a fluid (oil) which serves as an energy storage medium. The collectors are organized in 10 parallel loops placed along an east-west axis and are provided of a sun elevation tracking mechanism. The oil to be heated is extracted from the bottom of a storage tank and is pumped through the collector loops. At the other end, the outlet of the loops is collected in a passive pipe and brought back to the storage tank, where it enters at the top. The passive pipe introduces a long delay. The oil pump is provided with a local controller so that it can be assumed that oil flow is the manipulated variable, ranging from $2l/s$ to $9l/s$. The main process variable is the temperature of the oil entering the storage tank. In a cascade control

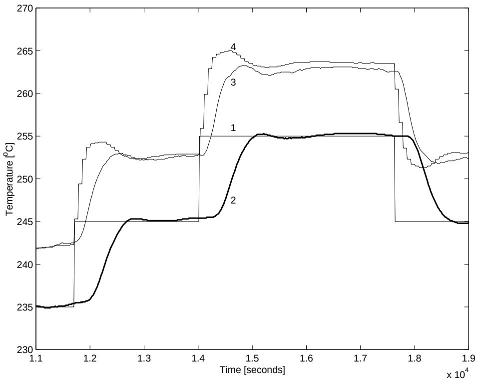

Fig. 4. Solar field: Temperature control using the MUSMAR multi-rate cascade algorithm.

framework, the average of the temperatures at the outlet of the loops is taken as the intermediate variable. In this way, the dynamics is decomposed in two parts: The dynamics of the collector loops, which relate the oil flow to $\overline{T}$; and the dynamics of the pipe connecting the outlet of the loops with the inlet of the storage tank, which relates the temperatures in both points. The former corresponds to the faster time constant (with a value of about 3 minutes). The latter corresponds to the slower time constant (in this case a pure delay of about 9 minutes in series with a time constant of about 2 minutes). With cascade control, the problems of rejecting disturbances in both subsystems are split apart.

Fig. 4 shows experimental results obtained with cascade multi-rate MUSMAR control. In this experiment both T_1 and T_2 (the prediction horizons on both MUSMAR controllers in fig.4) were made equal to 15 samples. This value was found from previous experiments and simulation to be adequate. The sampling intervals were $h_1 = 15\,sec$, $h_2 = 60\,sec$. When h_2 increases, the pure delay in P_2, measured in number of samples, decreases. The orders were set equal in both controllers and given by $n_i = 3$, $m_i = 2$. The control weight ρ_i is set equal to 0.001 in both controllers and the variance of the dither noise was 0.01. The pure delay is apparent in fig. 4, where the heat loss in the pipe connecting the outlet of the collector loops to the storage tank is also seen. The outer loop controller adjusts the set-point of the inner loop, such that y_1 is high enough to compensate for the thermal losses in the pipe and let the temperature at the inlet of the tank be equal to the set-point.

5. ARC WELDING CONTROL.

A schematic view of the experimental set-up used for the arc welding control example is shown in fig. 5. The objective of the arc welding control example is to lay a seam of soldier over a metallic piece, such that the rate of cooling (which determines the mechanical properties of the seam) is kept constant. The manipulated variable is the welding voltage. Further details

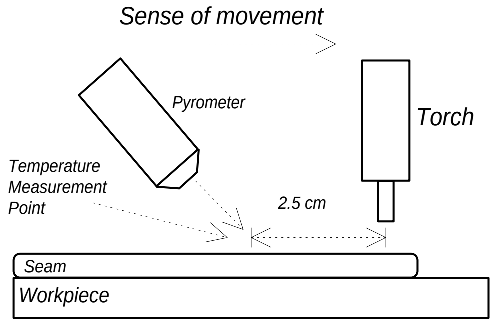

Fig. 5. Trailing centerline temperature measurement set-up.

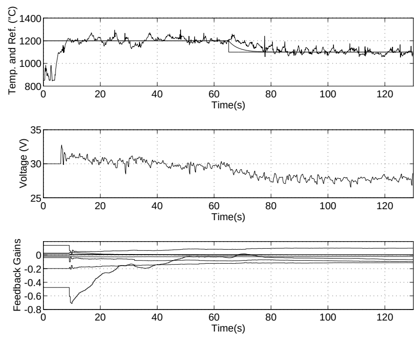

Fig. 6. Arc welding: Experimental results with MUSMAR on a $12\,mm$ plate.

and examples on the use of MUSMAR, as well as references on other types of approach may be found in (Santos, 2000). The dynamic behavior of the weld bead centerline temperature is modelled by a set of energy conservation equations describing the energy accumulation in the bead and in the workpiece. The dynamics is actually complex, being affected by various effects, including reflection of heat waves depending on the geometry of the pieces to weld. It may be shown (Santos *et al.*, 00, 2000) that it is impossible for a fixed gain controller to meet a robust stability specification, a fact naturally leading to an adaptive control approach.

The sampling frequency was chosen as $F_s = 3\,Hz$, the forgetting factor is $\lambda = 0.98$, the prediction horizon is $T = 10$ and the weight on the input penalty is $\rho = 500$. Results obtained on a $12\,mm$ piece show that MUSMAR is able to stabilize the plant yielding an acceptable performance. These are shown on fig. 6. In this example the value of ρ has the value $\rho = 2000$ in order to reduce excessive control action. In order to cancel the tracking offset, a parallel integrator has been inserted.

6. CONCLUSIONS.

This paper shows how MUSMAR, a predictive adaptive control algorithm based on multiple identifiers, can be used to tackle difficulties often found in industrial processes. These include high levels of uncertainty due to unmodelled plant dynamics, uncertain and/or time varying dynamics, fast acting strong disturbances and plants which may not be stabilized by controllers designed by minimizing single-step costs.

7. REFERENCES

Coito, F., J. M. Lemos, R. N. Silva and E. Mosca (1997). Adaptive Control of a solar energy plant: Exploiting accessible disturbances. *Int. J. Adaptive Control and Signal Proc.*, 11:327-342.

Greco, C., G. Menga, E. Mosca and G. Zappa (1984). Performance Improvements of Self-tuning Controllers by Multistep Horizons: The MUSMAR Approach. *Automatica*, 20:681-699.

Harris, T. (1989). Assessment of Control Loop Performance. *The Canadian J. Chem. Eng.*, 67:856-861.

Kulhavý, R. (1987). Restricted exponential forgetting in real-time identification, *Automatica*, 23(5):589-600.

Mosca, E. (1995). *Optimal, Predictive, and Adaptive Control*, Prentice Hall.

E. Mosca. G. Zappa. and J.M. Lemos (1989). ”Robustness of multipredictor adaptive regulators: MUSMAR” *Automatica*, 25:521 - 529.

T. O. Santos, R. B. Caetano, J. M. Lemos and F. J. Coito (2000). ”Multipredictive Adaptive Control of Arc Welding Trailing Centerline Temperature”. *IEEE Trans. Control Syst. Technology*, 8(1):159-169.

Silva, R. N., P. O. Shirley, J. M. Lemos and A. C. Gonçalves (2000). Adaptive regulation of superheated steam temperature: A case study in an industrial boiler. *Control Eng. Practice*, 8:1405-1415.